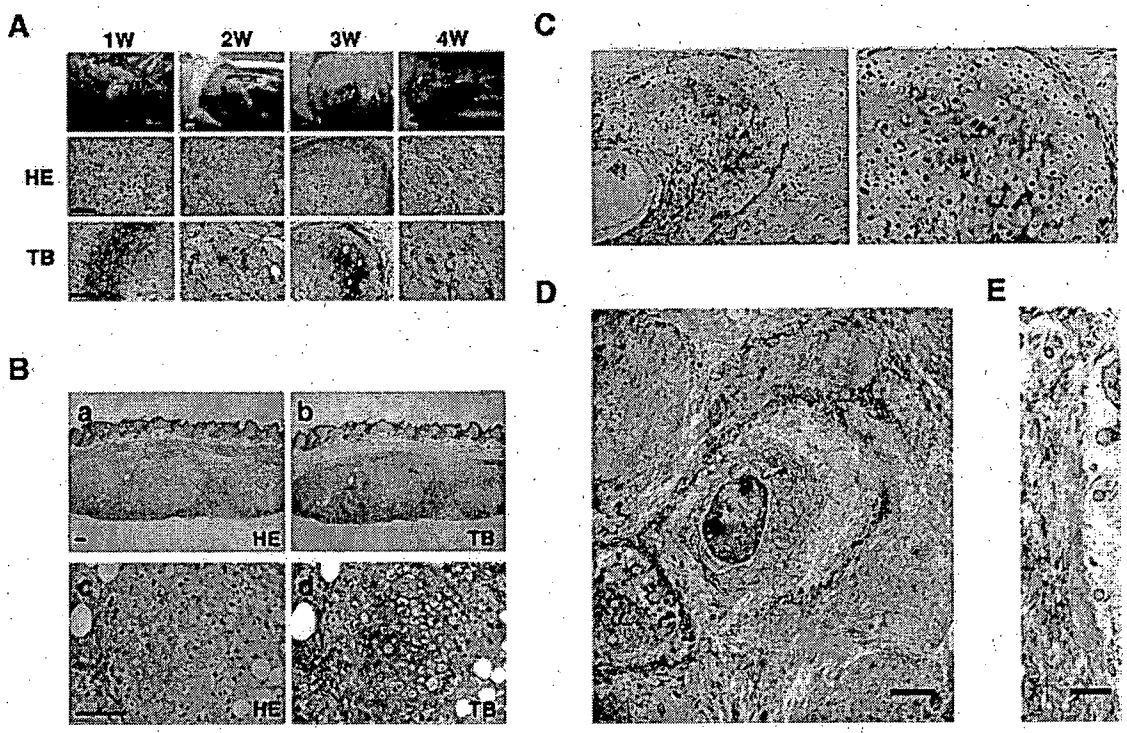

Fig. 6. In vivo chondrogenesis of KUM5 cells. **A:** Macroscopic view (**top**), hematoxylin and eosin stain (HE) (**middle**) and toluidine blue stain (TB) (**bottom**) analysis at 1, 2, 3, and 4 week (w)-cultivation in vivo after direct injection of KUM5 cells. **B:** KUM5 chondrogenic nodules, that were generated after pellet culture for 7 days in the CM supplemented with TGF-β3 and BMP2, were implanted just beneath the cutaneous muscle in the subcutaneous tissue and were cultivated in vivo for 3 weeks. **Panels c** and **d** are higher magnifications of **a** and **b**, respectively. **C:** Expression of chondrocyte-specific type II collagen. The KUM5 chondrogenic nodules were sectioned after 2 week-in vivo cultivation and stained with collagen type II-specific antibody. **D,E:** Ultrastructural analysis (TEM) of KUM5 implants. KUM5 cells were implanted into the subcutaneous tissue of Balb/c nu/nu mice, and the generated cartilage was resected 2 weeks after implantation. Scale bars: 2 mm (A, top row), 100 μm (A, middle and bottom row), 100 μm (B), 2 μm (D), 1 μm (E).

To determine the chondrogenic activity of OP9 cells in vivo, we directly injected them into the subcutaneous tissue. The OP9 cells without any induction did not generate cartilage. We then implanted the OP9 chondrogenic micromass after the pellet culture into the subcutaneous tissue just beneath the cutaneous muscle (Fig. 7A,B). The OP9 cartilage was formed at 2 and 4 weeks, and abundant metachromatic matrix was observed with the toluidine blue stain. The immunohistochemical analysis shows that OP9 cartilage stains positive for the chondrocyte-specific type II collagen (Fig. 7C).

Sorting of Chondroblasts by Chondrocyte-Specific Cis-Regulatory Element of the Collagen α2(XI) Gene

Although the KUM5 cells used in this study were derived from a single-cell origin or clone, it could be argued that both cells responsive and non-responsive to chondrogenic induction were present [Ko et al., 1990]. In this sense, KUM5 cells might have been a largely heterogeneous cell population. Even cells derived from a single clone have been shown to be heterogeneous in terms of differentiation capacity and stages [Muraglia et al., 2000]. To validate the chondrogenic differentiation observed here, a homogenous population of committed cell obtained after induction should be isolated. Therefore, for the purpose of sorting chondrogenically committed cells, we transfected KUM5 cells with a Venus-expression vector under the control of the Col α2(XI) promoter, analyzed the transfected cells, and collected Venus-positive cells (Fig. 8A–D). The sorted cells were assessed for in vitro (Fig. 9A–F) and in vivo chondrogenesis (Fig. 9G–I). The cells again showed metachromatic chondrogenic micromasses with toluidine blue staining in vitro (Fig. 9B). Direct injection of the cells resulted in the cartilage formation within 1 week and obvious enchondral ossification at the periphery

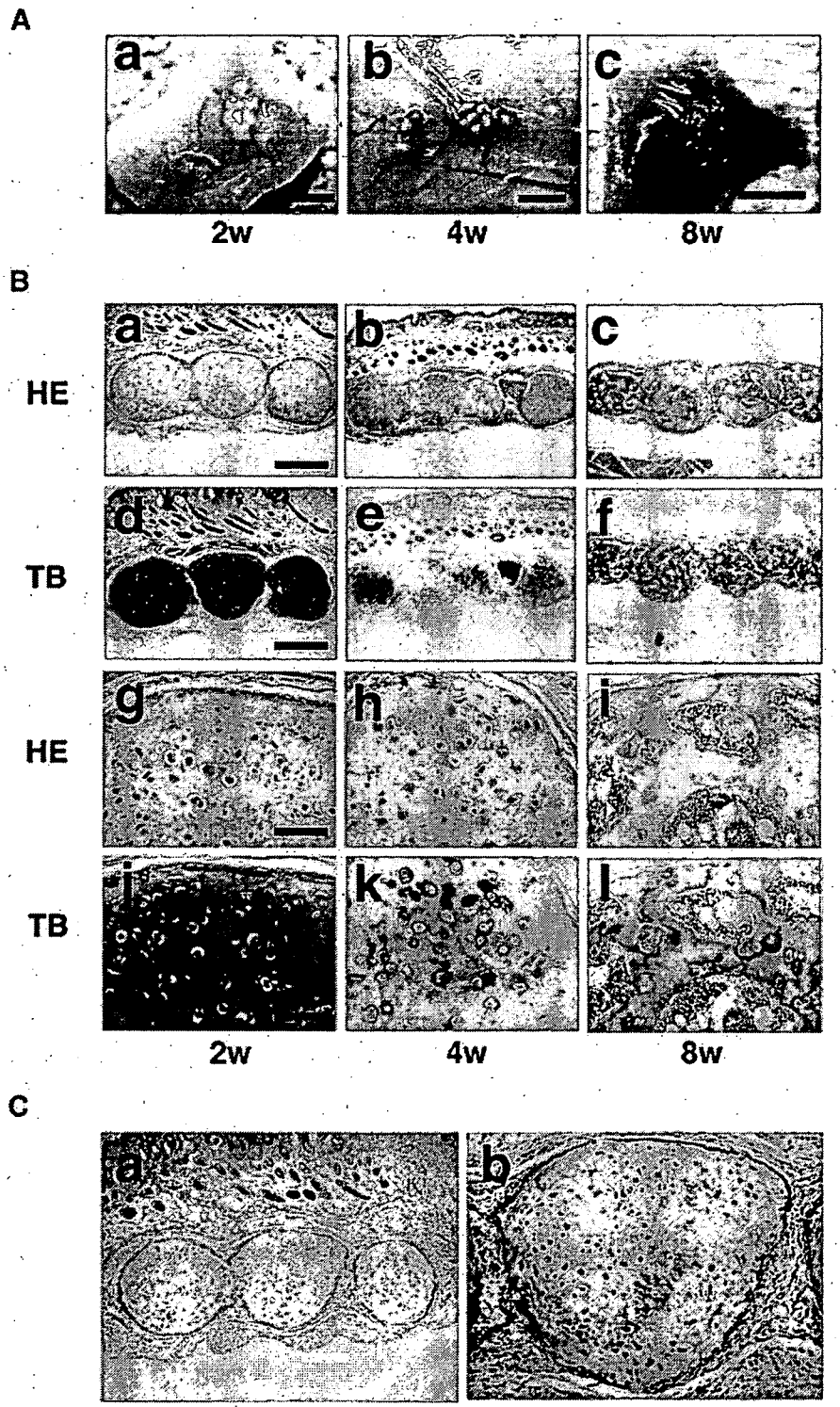

Fig. 7. In vivo chondrogenesis of OP9 cells. In vivo chondrogenesis was examined by implantation of OP9 chondrogenic nodules. OP9 chondrogenic nodules, which were generated after pellet culture for 7 days in the CM supplemented with TGF-β3 and BMP2, were implanted just beneath the cutaneous muscle in the subcutaneous tissue and were cultivated in vivo for the number of weeks indicated. **A**: Macroscopic view of OP9 cartilage after 2 (a), 4 (b), and 8 (c)-week-in vivo cultivation. **B**: Histological analysis of OP9 cartilage after 2 (**a,d,g,j**), 4 (**b,e,h,k**), and 8 (**c,f,i,l**)-week-in vivo cultivation. (a,b,c,g,h,i), HE stain; (d,e,f,j,k,l), TB stain. **Panels g–l** are higher magnifications of **a–f**, respectively. **C**: Immunohistochemical analysis of the in vivo OP9 chondrogenic nodules. The OP9 chondrogenic nodules after 2-week-in vivo cultivation stained positive for type II collagen. Scale bars: 2 mm (A), 500 μm (Ba–f), 100 μm (Bg–l).

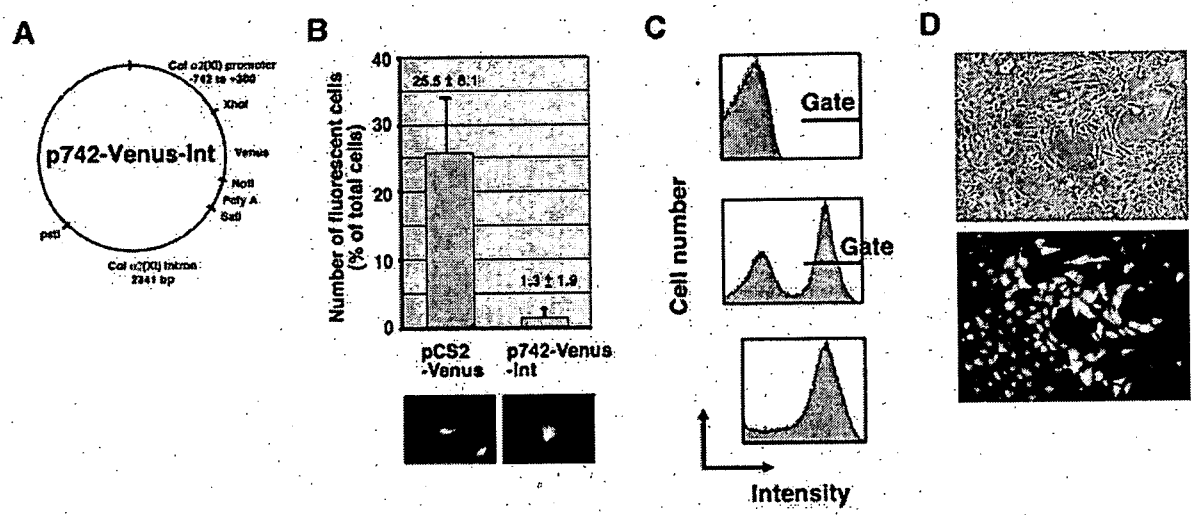

Fig. 8. Isolation of KUM5 chondroblasts using the chondroblast-specific cis-regulatory element. **A:** The p742-Venus-Int plasmid containing the fluorescent Venus gene driven by the cis-regulatory elements of the α2(XI) collagen gene. **B:** The number of fluorescent KUM5 cells (**upper**) after transfection with the p742-Venus-Int plasmid or pCS2-Venus containing the Venus gene driven by the CMV-promoter. Fluorescent photomicrograph of KUM5 cells after the first sorting (**lower**). **C:** Flowcytometric analysis of KUM5 cells after transfection with the p742-Venus-Int plasmid (**top**); The fluorescence-positive cells were sorted, propagated, and analyzed (**middle**). Again, the propagated fluorescence-positive cells were sorted, propagated, and analyzed (**bottom**). The "gate" for sorting is shown by the horizontal bar in the upper and middle panels. More than 80% of cells became positive after the final sorting. **D:** Phase contrast micrograph (upper) and fluorescent photomicrograph (lower) of the finally sorted cells (the lower panel of C).

of the cartilage at 4 weeks (Fig. 9G). Again, ultrastructural analysis revealed that KUM5 chondrocytes implanted into the subcutaneous tissue of nude mice were embedded in the hypertrophic chondrocytes and had abundant endoplasmic reticulum and a small number of mitochondria (Fig. 9H,I). The post-mitotic daughter cells in the cell nest, which are often observed in cartilage, were also detected (Fig. 9I).

DISCUSSION

In this study, we focus on the chondrogenic differentiation in vitro and in vivo using the two cell lines, KUM5 and OP9. The chondrogenic process is determined by the sequential expression of matrix component, and the differential response of differentiating cells to the growth factors may be attributed to the differentiating stages that depend on the expression patterns of the gene set as is the case for hematopoietic cells. The process of the chondrogenic differentiation is influenced by a number of growth factors including TGF-β and/or BMPs. Three isoforms of TGF-β have been known to have the ability to induce the chondrogenic differentiation. Both TGF-β2 and -β3 are more effective than TGF-β1 in promoting chondrogenesis, and TGF-β3 accelerates production of cartilaginous extracellular matrix in differentiating mesenchymal stem cells [Barry et al., 2001].

This study was undertaken to obtain mesenchymal stem cells with chondrogenic potential that retain critical in vivo cell functions, as do mammary gland epithelial cells, skin keratinocytes, and pigmented epithelial cells. To achieve this, we attempted to identify marrow-derived cells with chondrogenic nature and immortality without transformation among the cells obtained by the limiting-dilution method [Umezawa et al., 1992], defining "immortality" simply as indefinite cell division.

OP9 cells are known to serve as a niche or a specific microenvironment for the regulation of self-renewal and differentiation of stem cells [Nakano, 1996], and the question is raised of whether marrow stromal cells or marrow-derived mesenchymal cells with chondrogenic potential are capable of constituting a microenvironment for stem cells. It is inconceivable that cartilage can form a niche for cells in the living body based on structural and morphological considerations; however, a cell with chondrogenic or adipo-chondrogenic potential may serve as a niche not only in the case of OP9 cells but also as a general concept, at least in vitro.

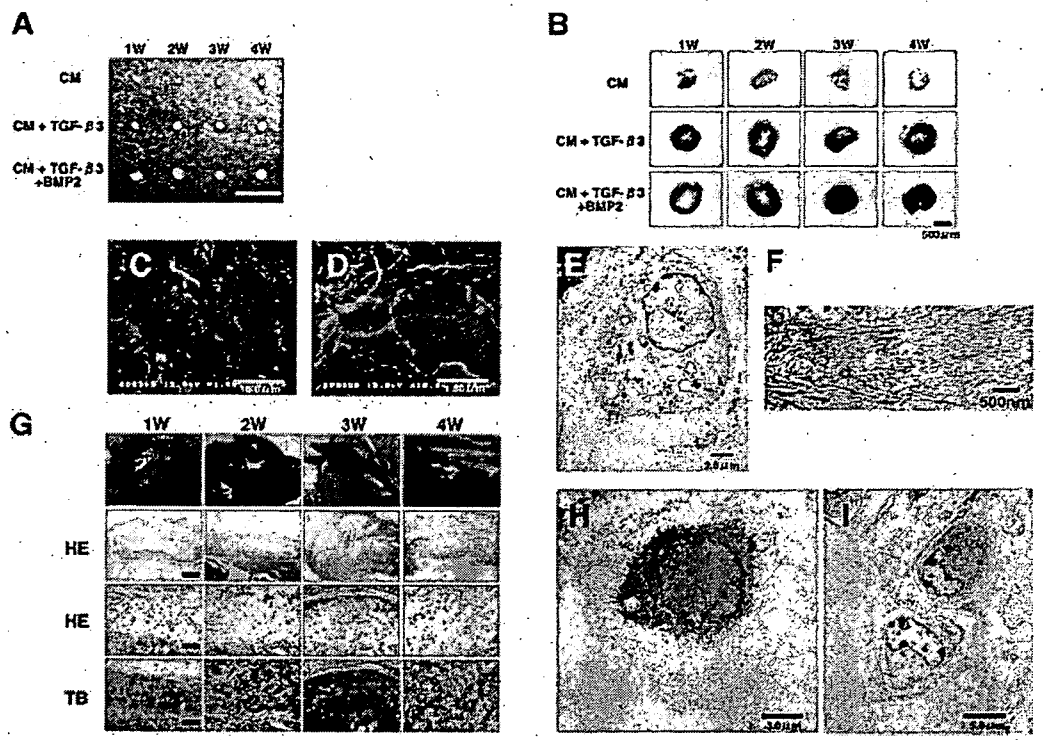

Fig. 9. In vitro and in vivo chondrogenesis of KUM5 cells sorted according to the activity of the chondrocyte-specific cis-regulatory element. **A,B:** Macroscopic view of the chondrogenic nodules which were generated after pellet culture of the finally sorted KUM5 cells for 1–4 weeks in the CM supplemented with growth factors as indicated (A) and toluidine blue stained section (B). **C–F:** Ultrastructural analysis of the micromasses of KUM5 cells sorted according to the activity of the Col α2(XI) cis-regulatory element (KUM5-Venus) after culturing in the CM supplemented with TGF-β3 for 3 weeks. (C,D), SEM; (E,F), TEM. **G:** In vivo chondrogenesis was examined 1–4 weeks after direct injection of the finally sorted KUM5 cells. From top to bottom: Macroscopic view, histological analysis, HE stain; histological analysis, HE stain; histological analysis, TB stain. **H,I:** Ultrastructural analysis (TEM) of the sorted KUM5 cartilage. The sorted KUM5 cells were implanted into the subcutaneous tissue of Balb/c nu/nu mice, and the generated cartilage was resected 2 weeks after implantation. Scale bars: 5 mm (A), 500 μm (B), 2 mm (G, **top row**), 500 μm (G, **2nd row**), 100 μm (G, **3rd** and **bottom row**).

The sequence of enchondral or perichondral ossification by KUM5 and OP9 cells was as follows: deposition of homogeneous matrix surrounding the small nests of the injected cells that subsequently became positive for type II collagen and exhibited metachromasia with toluidine blue staining, trapping them in the secreted homogeneous matrix, and the appearance of small nests of isogenous chondrocytes that probably resulted from repeated cell division. At a later stage, that is, 4–8 weeks after injection, the peripheral region of the generated cartilage became ossified. Importantly, the chondrogenesis by KUM5 and OP9 cells was irreversible and reproducible, and the implanted cells never transformed into malignant cells, formed any abnormal extracellular matrices, or induced any significant inflammatory reactions. It is again noteworthy that the osteogenesis by these two different lines of cells was mediated by chondrogenesis, and it was therefore considered to be chondral ossification. Thus, the unique characteristics of these two cell lines provide an opportunity to analyze the process of enchondral or perichondral ossification in an experimental system in detail.

In fetal life, primary ossification centers form by one of two processes: enchondral ossification or membranous ossification. Enchondral ossification refers to bony replacement of cartilage and is the mode of formation of the long bones. During membranous ossification mesenchymal cells form membranes within which ossification occurs and this is the mode of formation of the scapula and skull and, in part, of the clavicle and pelvis. After birth, bone growth continues by both enchondral and membranous ossification. Further enchondral ossification occurs in

the physes and results in continuous longitudinal growth of the long bones until skeletal maturity. KUM5 and OP9 cells were obtained from long bone and calvaria, respectively, and showed enchondral ossification. We have also reported that KUSA-A1 cells form bone by membranous ossification in vivo, and thus we have three different types of cells showing distinctive in vivo characteristics. The process of chondrogenesis or enchondral ossification may also serve as a model for chondromatosis and osteochondromatosis in a joint cavity.

The expression pattern of chondrocyte-specific genes in OP9 and KUM5 cells is different from that in ATDC5 cells, which are a mouse embryonal carcinoma-derived chondrogenic cell line. ATDC5 cells exhibit a multistep differentiation process encompassing the stages from chondrogenesis to enchondral ossification [Shukunami et al., 1996]. Early-phase differentiation is characterized by the expression of type II collagen, followed by induction of the aggrecan gene. Late stage differentiation is characterized by the start of expression of short-chain collagen type X genes. By contrast, marrow-derived mesenchymal stem cells express the aggrecan genes at an early stage and then type II collagen during chondrogenic differentiation [Pittenger et al., 1999]. Surprisingly, gene expression pattern determined by the gene chip analysis was consistent with protein levels of cell surface molecules; this consistency indicates that the expression profiling is valid. Expression of "structural proteins" on Gene Ontology, including the extracellular matrix, was much higher by OP9 and KUM5 cells than by non-chondrogenic cells such as KUSA-A1 osteoblasts, H-1/A preadipocytes, and 9-15c mesenchymal stem cells, implying that the OP9 and KUM5 cells are mainly engaged in synthesizing extracellular matrix.

Can we inhibit enchondral or perichondral ossification after the completion of chondrogenesis? This is a challenge for the future, probably the not-too-distant future. We could not prevent the generated hyaline cartilage from ossifying at present even after selection based on the chondrocyte-specific cis-regulatory element of the collagen α2(XI) gene, probably due to the inability to inhibit vasculogenesis from the neighboring connective tissue. However, these established murine marrow-derived mesenchymal cells with in vivo chondrogenic activity and expression profiles provide a powerful model for studies of chondrogenic differentiation and our further understanding of cartilage regeneration. Bone marrow-derived chondroblasts with chondrogenic potential are useful candidate cell sources in addition to dedifferentiated chondrocytes obtained from cartilage for transplantation in osteoarthritis and rheumatoid arthritis.

ACKNOWLEDGMENTS

We would like to express our sincere thanks to Shin-ichiro Takayama, Yasushi Nakao, Hiroyasu Ikegami, and Toshiyasu Nakamura for support throughout the work, Atsushi Miyawaki for the Venus/pCS2 plasmid, Kayoko Saito for secretarial assistance, and Toshihiro Nagai and Yoshie Hashimoto for providing expert technical assistance. This study was supported by grants from the Ministry of Education, Culture, Sports, Science, and Technology (MEXT) of Japan, the Health; Labour Sciences Research Grants, and the Pharmaceuticals and Medical Devices Agency; by Research on Health Science focusing on Drug Innovation (KH71064) from the Japan Health Science Foundation; by the program for promotion of fundamental Studies in Health Science of the Pharmaceuticals and Medical Devices Agency (PMDA); by the research Grant for Cardiovascular Disease (H16C-6) from the ministry of Health, Labour and Welfare; by supported by a Grant for Child Health and Development (H15C-2) from the Ministry of Health, Labour and Welfare. The raw data from the gene chip analysis is available at our laboratory's web site (http://1954.jukuin.keio.ac.jp/umezawa/chip/sugiki/index.html). The photomicrographs of the pelleted micromasses examined by SEM and TEM were available at http://1954.jukuin.keio.ac.jp/umezawa/sugiki/EM/index.html. The wrl files of the 3D-representation of PCA are available at http://1954.jukuin.keio.ac.jp/umezawa/sugiki/pca/index.html.

REFERENCES

Archer CW, McDowell J, Bayliss MT, Stephens MD, Bentley G. 1990. Phenotypic modulation in sub-populations of human articular chondrocytes in vitro. J Cell Sci 97(Pt 2):361–371.

Barry F, Boynton RE, Liu B, Murphy JM. 2001. Chondrogenic differentiation of mesenchymal stem cells from bone marrow: Differentiation-dependent gene expression of matrix components. Exp Cell Res 268:189–200.

Benya PD, Shaffer JD. 1982. Dedifferentiated chondrocytes reexpress the differentiated collagen phenotype when cultured in agarose gels. Cell 30:215–224.

Bianco P, Robey PG. 2000. Marrow stromal stem cells. J Clin Invest 105:1663–1668.

Bonaventure J, Kadhom N, Cohen-Solal L, Ng KH, Bourguignon J, Lasselin C, Freisinger P. 1994. Reexpression of cartilage-specific genes by dedifferentiated human articular chondrocytes cultured in alginate beads. Exp Cell Res 212:97–104.

Fujii M, Takeda K, Imamura T, Aoki H, Sampath TK, Enomoto S, Kawabata M, Kato M, Ichijo H, Miyazono K. 1999. Roles of bone morphogenetic protein type I receptors and Smad proteins in osteoblast and chondroblast differentiation. Mol Biol Cell 10:3801–3813.

Hauselmann HJ, Fernandes RJ, Mok SS, Schmid TM, Block JA, Aydelotte MB, Kuettner KE, Thonar EJ. 1994. Phenotypic stability of bovine articular chondrocytes after long-term culture in alginate beads. J Cell Sci 107: 17–27.

Johnstone B, Hering TM, Caplan AI, Goldberg VM, Yoo JU. 1998. In vitro chondrogenesis of bone marrow-derived mesenchymal progenitor cells. Exp Cell Res 238:265–272.

Ko MS, Nakauchi H, Takahashi N. 1990. The dose dependence of glucocorticoid-inducible gene expression results from changes in the number of transcriptionally active templates. EMBO J 9:2835–2842.

Kohyama J, Abe H, Shimazaki T, Koizumi A, Nakashima K, Gojo S, Taga T, Okano H, Hata J, Umezawa A. 2001. Brain from bone: Efficient "meta-differentiation" of marrow stroma-derived mature osteoblasts to neurons with Noggin or a demethylating agent. Differentiation 68:235–244.

Lefebvre V, Peeters-Joris C, Vaes G. 1990. Production of collagens, collagenase and collagenase inhibitor during the dedifferentiation of articular chondrocytes by serial subcultures. Biochim Biophys Acta 1051:266–275.

Maeda S, Hayashi M, Komiya S, Imamura T, Miyazono K. 2004. Endogenous TGF-beta signaling suppresses maturation of osteoblastic mesenchymal cells. EMBO J 23:552–563.

Makino S, Fukuda K, Miyoshi S, Konishi F, Kodama H, Pan J, Sano M, Takahashi T, Hori S, Abe H, Hata J, Umezawa A, Ogawa S. 1999. Cardiomyocytes can be generated from marrow stromal cells in vitro. J Clin Invest 103:697–705.

Mori T, Kiyono T, Imabayashi H, Takeda Y, Tsuchiya K, Miyoshi S, Makino H, Matsumoto K, Saito H, Ogawa S, Sakamoto M, Hata J, Umezawa A. 2005. Combination of hTERT and bmi-1, E6, or E7 induces prolongation of the life span of bone marrow stromal cells from an elderly donor without affecting their neurogenic potential. Mol Cell Biol 25:5183–5195.

Muraglia A, Cancedda R, Quarto R. 2000. Clonal mesenchymal progenitors from human bone marrow differentiate in vitro according to a hierarchical model. J Cell Sci 113(Pt 7):1161–1166.

Nagai T, Ibata K, Park ES, Kubota M, Mikoshiba K, Miyawaki A. 2002. A variant of yellow fluorescent protein with fast and efficient maturation for cell-biological applications. Nat Biotechnol 20:87–90.

Nakano T. 1996. In vitro development of hematopoietic system from mouse embryonic stem cells: A new approach for embryonic hematopoiesis. Int J Hematol 65:1–8.

Nakano T, Kodama H, Honjo T. 1994. Generation of lymphohematopoietic cells from embryonic stem cells in culture. Science 265:1098–1101.

Ochi K, Chen G, Ushida T, Gojo S, Segawa K, Tai H, Ueno K, Ohkawa H, Mori T, Yamaguchi A, Toyama Y, Hata J, Umezawa A. 2003. Use of isolated mature osteoblasts in abundance acts as desired-shaped bone regeneration in combination with a modified poly-DL-lactic-co-glycolic acid (PLGA)-collagen sponge. J Cell Physiol 194: 45–53.

Pittenger MF, Mackay AM, Beck SC, Jaiswal RK, Douglas R, Mosca JD, Moorman MA, Simonetti DW, Craig S, Marshak DR. 1999. Multilineage potential of adult human mesenchymal stem cells. Science 284:143–147.

Reginato AM, Iozzo RV, Jimenez SA. 1994. Formation of nodular structures resembling mature articular cartilage in long-term primary cultures of human fetal epiphyseal chondrocytes on a hydrogel substrate. Arthritis Rheum 37:1338–1349.

Shukunami C, Shigeno C, Atsumi T, Ishizeki K, Suzuki F, Hiraki Y. 1996. Chondrogenic differentiation of clonal mouse embryonic cell line ATDC5 in vitro: Differentiation-dependent gene expression of parathyroid hormone (PTH)/PTH-related peptide receptor. J Cell Biol 133: 457–468.

Terai M, Uyama T, Sugiki T, Li XK, Umezawa A, Kiyono T. 2005. Immortalization of human fetal cells: The life span of umbilical cord blood-derived cells can be prolonged without manipulating p16INK4a/RB breaking pathway. Mol Biol Cell 16:1491–1499.

Tsumaki N, Kimura T, Matsui Y, Nakata K, Ochi T. 1996. Separable cis-regulatory elements that contribute to tissue- and site-specific alpha 2(XI) collagen gene expression in the embryonic mouse cartilage. J Cell Biol 134:1573–1582.

Umezawa A, Tachibana K, Harigaya K, Kusakari S, Kato S, Watanabe Y, Takano T. 1991. Colony-stimulating factor 1 expression is down-regulated during the adipocyte differentiation of H-1/A marrow stromal cells and induced by cachectin/tumor necrosis factor. Mol Cell Biol 11:920–927.

Umezawa A, Maruyama T, Segawa K, Shadduck RK, Waheed A, Hata J. 1992. Multipotent marrow stromal cell line is able to induce hematopoiesis in vivo. J Cell Physiol 151:197–205.

Cell Tissue Res
DOI 10.1007/s00441-006-0257-6

REGULAR ARTICLE

Establishment of immortalized dental follicle cells for generating periodontal ligament in vivo

T. Yokoi · M. Saito · T. Kiyono · S. Iseki · K. Kosaka · E. Nishida · T. Tsubakimoto · H. Harada · K. Eto · T. Noguchi · T. Teranaka

Received: 23 January 2006 / Accepted: 24 May 2006

Abstract The dental follicle is a mesenchymal tissue that surrounds the developing tooth germ. During tooth root formation, periodontal components, viz., cementum, periodontal ligament (PDL), and alveolar bone, are created by dental follicle progenitors. Here, we report the presence of PDL progenitors in mouse dental follicle (MDF) cells. MDF cells were obtained from mouse incisor tooth germs and immortalized by the expression of a mutant human papilloma virus type 16 *E6* gene lacking the PDZ-domain-binding motif. MDF cells expressing the mutant *E6* gene ($MDF^{E6\text{-}EGFP}$ cells) had an extended life span, beyond 150 population doublings (PD). In contrast, normal MDF cells failed to proliferate beyond 10 PD. $MDF^{E6\text{-}EGFP}$ cells expressed tendon/ligament phenotype-related genes such as *Scleraxis* (*Scx*), *growth and differentiation factor-5*, *EphA4*, *Six-1*, and *type I collagen*. In addition, the expression of *periostin* was observed. To elucidate the differentiation capacity of $MDF^{E6\text{-}EGFP}$ cells in vivo, the cells were transplanted into severe combined immunodeficiency mice. At 4 weeks, $MDF^{E6\text{-}EGFP}$ cell transplants had the capacity to generate a PDL-like tissue that expressed *periostin*, *Scx*, and *type XII collagen* and the fibrillar assembly of type I collagen. Our findings suggest that $MDF^{E6\text{-}EGFP}$ cells can act as PDL progenitors, and that these cells may be a useful research tool for studying PDL formation and for developing regeneration therapies.

Keywords Dental follicle · Progenitor · Development · Immortalization · Periodontal ligament · Mouse (ICR)

This work was supported by a Grant-in Aid for the High-Tech Research Center Project from the Ministry of Education, Culture, Sports, Science, and Technology of Japan, the AGU High-Tech Research Center Project, the 2003-Multidisciplinary Research Project from MEXT, and grants from the Ministry of Education, Culture, Sports, Science, and Technology of Japan.

T. Yokoi · M. Saito (✉) · K. Kosaka · E. Nishida · T. Tsubakimoto · T. Teranaka
Department of Medicine,
Division of Operative Dentistry and Endodontics,
Kanagawa Dental College,
82 Inaoka-cho,
Yokosuka, Kanagawa 238-8580, Japan
e-mail: saitohms@kdcnet.ac.jp

T. Yokoi · E. Nishida · T. Noguchi
Department of Periodontology, School of Dentistry,
Aichi-gakuin University,
Nagoya, Aichi, Japan

M. Saito
Oral Health Science Research Center, Kanagawa Dental College,
Yokosuka, Kanagawa, Japan

T. Kiyono
Virology Division, National Cancer Research Institute,
Tokyo, Japan

S. Iseki · K. Eto
Department of Molecular Craniofacial Embryology,
Graduate School, Tokyo Medical and Dental University,
Tokyo, Japan

H. Harada
Department of Oral Anatomy and Developmental Biology,
Osaka University Graduate School of Dentistry,
Suita, Osaka, Japan

Introduction

The periodontal ligament (PDL), which surrounds the tooth root, absorbs occlusal forces and functions as a sense organ (Ten Cate 1994). In periodontitis, a chronic inflammatory disease, the PDL is irreversibly damaged. Despite a number of novel approaches, no one has yet succeeded in reliably forming PDL (D'Errico et al. 1999).

Hence, there is considerable interest in the developmental mechanisms of PDL.

The PDL originates from dental follicle cells formed during the cap stage of tooth germ development by an ectomesenchymal progenitor cell population originating from cranial neural crest cells (Chai et al. 2000). Progenitors in the dental follicle are thought to contribute to the formation of all periodontal tissues, namely cementum, PDL, and alveolar bone (Bosshardt and Schroeder 1996). After the formation of tooth root dentin, cementoblast progenitors in the dental follicle migrate onto the tooth root surface and differentiate into cementoblasts (Bosshardt and Schroeder 1996). Almost simultaneously, PDL progenitors within the dental follicle cells differentiate into PDL cells. Finally, both bone- and PDL-derived fibers coalesce in the PDL to form the intermediate plexus. Although a specific marker for PDL is not available, tendon/ligament phenotype-related genes are thought to be involved in the differentiation of PDL progenitors. Growth and differentiation factors (GDFs)-5, 6, and 7 are members of the bone morphogenetic protein family that regulate tendon/ligament formation (Wolfman et al. 1997) and have been shown to be expressed by both dental follicle and PDL cells (Morotome et al. 1998; Nakamura et al. 2003; Sena et al. 2003). Screlaxis (*Scx*), a basic helix-loop-helix transcription factor that serves as a tendon progenitor marker gene, has also been found to be expressed by PDL stem cells (Brent et al. 2003; Seo et al. 2004). Non-collagenous extracellular matrix has been shown to be involved in the formation of PDL (Matias et al. 2003). *Periostin* is a marker for preosteoblasts but is also found in the periosteum and PDL (Horiuchi et al. 1999). During tooth germ development, *periostin* is initially expressed in the dental follicle cells and is then restricted to postnatal PDL cells during tooth root formation (Kruzynska-Frejtag et al. 2004). *Periostin-/-* mice develop a periodontal-disease-like phenotype within 3 months of birth, suggesting that this protein plays a critical role in maintenance of the PDL (Rios et al. 2005). These findings suggest that both tendon/ligament phenotype-related genes and extracellular matrices, which are highly expressed in PDL, are involved in PDL formation and maintenance. However, details of the mechanisms involved in PDL formation are yet to be clarified, because of the scarcity of PDL progenitor culture systems.

Recently, we have demonstrated the presence of cementoblast progenitors in bovine dental follicle cells (Handa et al. 2002). A cementoblast progenitor cell line, designated as BCPb8, has the capacity to form PDL- and cementum-like tissue when transplanted into severe combine immunodeficiency (SCID) mice (Saito et al. 2005). Although BCPb8 is a clonal cell line useful for the study of dental follicle progenitors, the use of these cells derived from a bovine species is restricted, because the cDNA database is inadequate, and because antibodies are limited. Thus, little is known about the biological properties of dental follicle progenitors or the mechanisms that regulate their differentiation. Investigations directed at addressing these key questions are essential if we are to understand the developmental mechanisms of PDL. In this study, we have attempted to establish immortalized mouse dental follicle (MDF) cells for the study of progenitors in dental follicle cells.

Materials and methods

Tissue culture

MDF cells were isolated from the dental follicle tissue of the incisor tooth germs of 1-day postnatal (P1) ICR mice. Briefly, mouse dental follicle tissue was mechanically stripped from the lingual posterior region of mouse incisor and placed onto a 24 multi-well plate. The tissues were then incubated with α-minimum essential medium (α-MEM: Sigma, St. Louis, USA) containing 10% fetal bovine serum (FBS; BioWhittaker, Maryland, USA), 50 μg/ml ascorbic acid, 100 U/ml streptomycin and penicillin, in a humidified atmosphere of 5% CO_2 at 37°C. When the cells reached approximately 80% confluence, they were passaged with 0.25% trypsin/1 mM EDTA and maintained as MDF cells. These cells were plated into six wells at a density of 3×10^4 cells/ml, and the medium was changed every 2 days.

Infection of retrovirus constructs and establishment of $MDF^{E6\text{-}EGFP}$ cells

The construction of pCLXSN-$16E6^{\Delta146\text{-}151}$ and the production of LXSN-$16E6^{\Delta146\text{-}151}$ retrovirus have been described previously (Kyo et al. 2003). An aliquot of 1 ml producer cell culture fluid was added to MDF cells (passage 1) in the presence of polybrene (8 μg/ml), and the cells were subsequently selected in the presence of G418 (100 μg/ml). Transduced cells were maintained in the medium described above. Following infection with LXSN-$16E6^{\Delta146\text{-}151}$, MDF cells were transduced with EGFP lentivirus under the control of a CMV promoter to obtain stably expressed EGFP ($MDF^{E6\text{-}EGFP}$).

Osteogenic differentiation

Cells were plated into six wells at a density of 3×10^4 cells/ml and cultured in the medium described above supplemented with 100 nM dexamethasone, 50 μg/ml ascorbic acid, 10 mM β-glycerophosphate. The culture medium was

replaced every 2 days, and the cells were maintained for 3 weeks.

Alkaline phosphatase activity and alizarin red staining

To evaluate alkaline phosphatase (ALP) activity, $MDF^{E6\text{-}EGFP}$ cells were fixed with 4% paraformaldehyde for 20 min at 21°C. After being washed with PBS, the cells were incubated for 20 min in a mixture of 0.1 mg/ml naphthol AS-MX phosphate (Sigma), 0.5% N-N dimethyl formamide (Sigma), 2 mM $MgCl_2$, 0.6 mg/ml Fast Blue BB salt (Sigma) in 0.1 M TRIS-HCl (pH 8.5) at room temperature. Calcium accumulation was detected by staining preparations with 2% alizarin red S (pH 6.4) (Sigma). MC3T3E1 (purchased from RIKEN BioResource Center, Japan) and NIH3T3 were used as controls.

Probes for in situ hybridization

The cDNA of mouse *osteopontin* open reading frame (885 bp), mouse *Scx* 3′ untranslated region (UTR; 291 bp), or mouse *type XII collagen* (500 bp) region was amplified by reverse transcription/polymerase chain reaction (RT-PCR) by using the following primers: *osteopontin*, 5′-ATGAGATTGGCAGTGATTTG-3′ and 5′-GTTGACCT CAGAAGATGAAC-3′; *Scx*, 5′-AAGAGGT GATGCCAC TAGTG-3′and 5′-TATACAAAATTTCCA GACTTTAT ATTATCAT-3′; *type XII collagen*, 5′-TCCCCATCAAA GAACAGACC-3′ and 5′-TGACTGCTGGATGA CAAAGG-3′. The amplicons for *osteopontin* and *Scx* were subsequently cloned into the pCRII vector (Invitrogen, Carlsbad, Calif., USA), and those for *type XII collagen* were cloned into pCR 4-TOPO (Invitrogen). A 623-bp mouse *periostin* cDNA fragment was isolated by RT-PCR with partial T7 and T3 promoter-containing primers (below, in italics) at the 5′ end and the 3′ end, respectively: T7: 5′-*CACTATAGGGC*GGCTGAA GATGGTTCCTCTC-3′, and T3: 5′-*CACTAAAGGG*GC CATGTGGCTGTGTAAGG CATTC-3′. These cDNA fragments were further amplified by using the following adaptor primers to install full T7 and T3 promoter sequences into the fragments: 5′-GTAATAC GACTCAC TATAGGGC-3′ for T7, and 5′-AAT TAACCCTCAC TAAAGG-3′ for T3.

In situ hybridization

To generate antisense and sense digoxygenin-labeled riboprobes, linearized *osteopontin*, *Scx*, and *type XII collagen* plasmids and *periostin* cDNA fragments (see previous section) were transcribed by T7, T3, or Sp6 RNA polymerase as described elsewhere (Wilkinson 1995). Heads of P1 C57BL/6 mice were embedded in OCT compound (Sakura Finetechnical, Tokyo, Japan), and 10-μm-thick sagittal sections were cut. Mandibles of P35 mice were fixed in 4% paraformaldehyde at 4°C overnight, decalcified in 12.5% EDTA containing 2.5% paraformaldehyde for 6 weeks, and then embedded in OCT compound. In situ hybridization was carried out on these sections as previously described with some modification (Iseki et al. 1999). Polyvinyl alcohol was used as buffer during the color reaction.

RNA preparation and RT-PCR

Total RNA was isolated from cells by using ISOGEN (Nippon Gene, Tokyo, Japan) as described previously (Handa et al. 2002). cDNAs were synthesized from 1 μg total RNA in a 20-μl reaction volume containing 10× reaction buffer, 1 mM dNTP mixture, 1 U/μl RNase inhibitor, 0.25 U/μl reverse transcriptase (M-MLV reverse transcriptase; Invitrogen), and 0.125 μM random 9-mers (Takara, Tokyo, Japan). Amplification was performed in a PCR Thermal Cycler SP (Takara, Tokyo, Japan) for 25 cycles with the following reaction profile: 94°C for 1 min, 60°C for 30 s, and 72°C for 30 s. Synthesized cDNA served as a template for subsequent PCR amplification with mouse-specific primers: *bone sialoprotein* (*BSP*): sense 5′-AGGGAACTGACCAGTGTTGG-3′, antisense 5′-TCGTTGCCTGTTTGTTCGTA-3′; *osteocalcin* (*OC*): sense 5′-CATGAGGACCCTCTCTCTGC-3′, antisense 5′-GCCGGAGTCTGTTCACTACC-3′; *osteopontin*: sense 5′-TGCACCCAGATCCTATGACC-3′, antisense 5′-TGTGGTCATGGCTTTCATTG-3′; *periostin*: sense 5′-TTGAAGGTGTCCCGSCTTC-3′, antisense 5′-TGAT TCGTTCTTCCCGAGTC-3′; *Scx*: sense 5′-CTTTCTTC CACAAGCGGTCGT-3′, antisense 5′-TGTCACGGTCTT TGCTCAAC-3′; and *glyceraldehyde-3-phosphate dehydrogenase* (*GAPDH*): sense 5′-TGTTCCTACCCCCAA TTGTGT-3′, antisense 5′-AGGAGACAACCTGGTCC TCA-3′. Specific primers for *six-1*, *EphA4*, *GDF-5*, *collagen I* (*Coll*), and *osterix* have been described previously (Salingcarnboriboon et al. 2003).

In vivo differentiation assay

The differentiation potential of $MDF^{E6\text{-}EGFP}$ cells was assessed by transplantation of the cells into SCID mice as described previously (Handa et al. 2002). Briefly, cells were inoculated subcutaneously into 5-week-old male CB-17 scid/scid (SCID) mice (Nihoncrea, Tokyo, Japan) after incubation of 1.5×10^6 cells in a mixture of 40 mg hydroxyapatite powder (Osferion, Olympus, Tokyo, Japan) and fibrin clot (mixture of mouse fibrinogen and thrombin: both from Sigma). Transplantation analysis was carried out three times, and three transplants were prepared per group. The mice were sacrificed after 4 weeks and subjected to

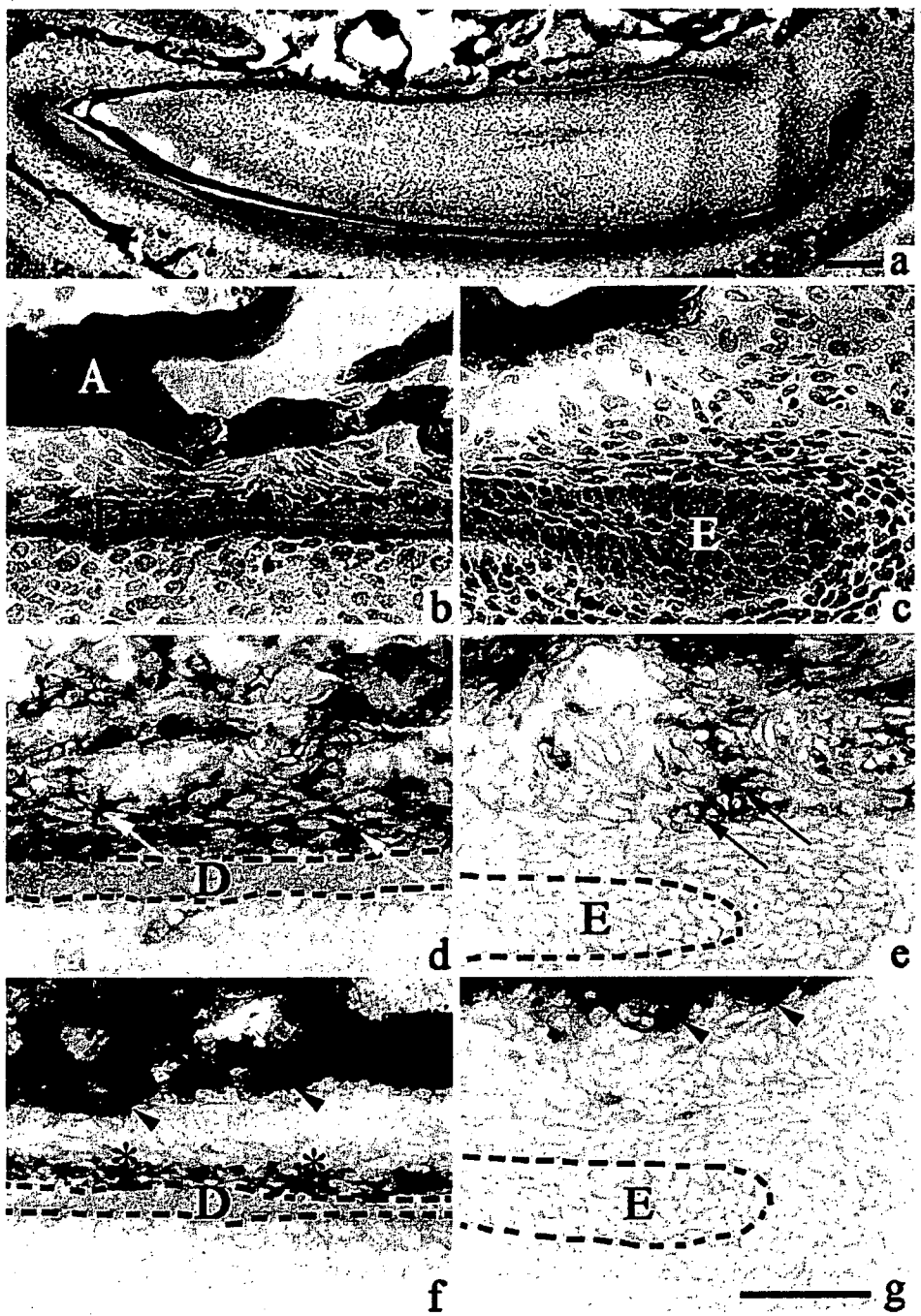

Fig. 1 In situ hybridization for *periostin* and *osteopontin* mRNA in newborn mice (*A* alveolar bone, *D* dentin, *E* dental epithelium). Sagittal sections of the incisor in the lower jaw of P1 mouse (**a**) were examined by hematoxylin and eosin staining (**a–c**) or in situ hybridization for *periostin* (**d, e**) or *osteopontin* (**f, g**). Higher magnifications of the anterior (**b, d, f**) and posterior (**c, e, g**) regions of the lingual side of the incisor are shown. Intense expression of *periostin* is seen in the developing PDL in the anterior region (**d**, *arrows*), with little expression in the posterior region (**e**, *arrows*). *Osteopontin* is expressed strongly throughout the alveolar bone (**f, g**, *arrowheads*) and in the differentiated cementoblasts in the anterior region (**f**, *asterisks*). No expression of *osteopontin* is observed in the dental follicle tissue in the posterior region (**g**). *Bars* 100 μm

histochemical analysis with immunohistochemical staining or in situ hybridization as described below. NIH3T3 cells were used for comparison.

Histochemical analysis

The transplants were fixed in 4% paraformaldehyde for 1 day, decalcified with 12.5% EDTA containing 2.5% paraformaldehyde for 3 days, and then embedded in OCT compound for the production of frozen sections. Subsequently, 30 serial sections of 5 μm in thickness were cut per implant and analyzed histochemically. Morphology was examined by hematoxylin and eosin staining. Observation by fluorescence microscopy (Axio imager, Carl Zeiss, Germany) was performed to distinguish between the cells of donor origin and host tissue. Expression of mRNA for *periosotin* and *Scx* was examined by in situ hybridization as described above. For immunohistocemical analysis, the

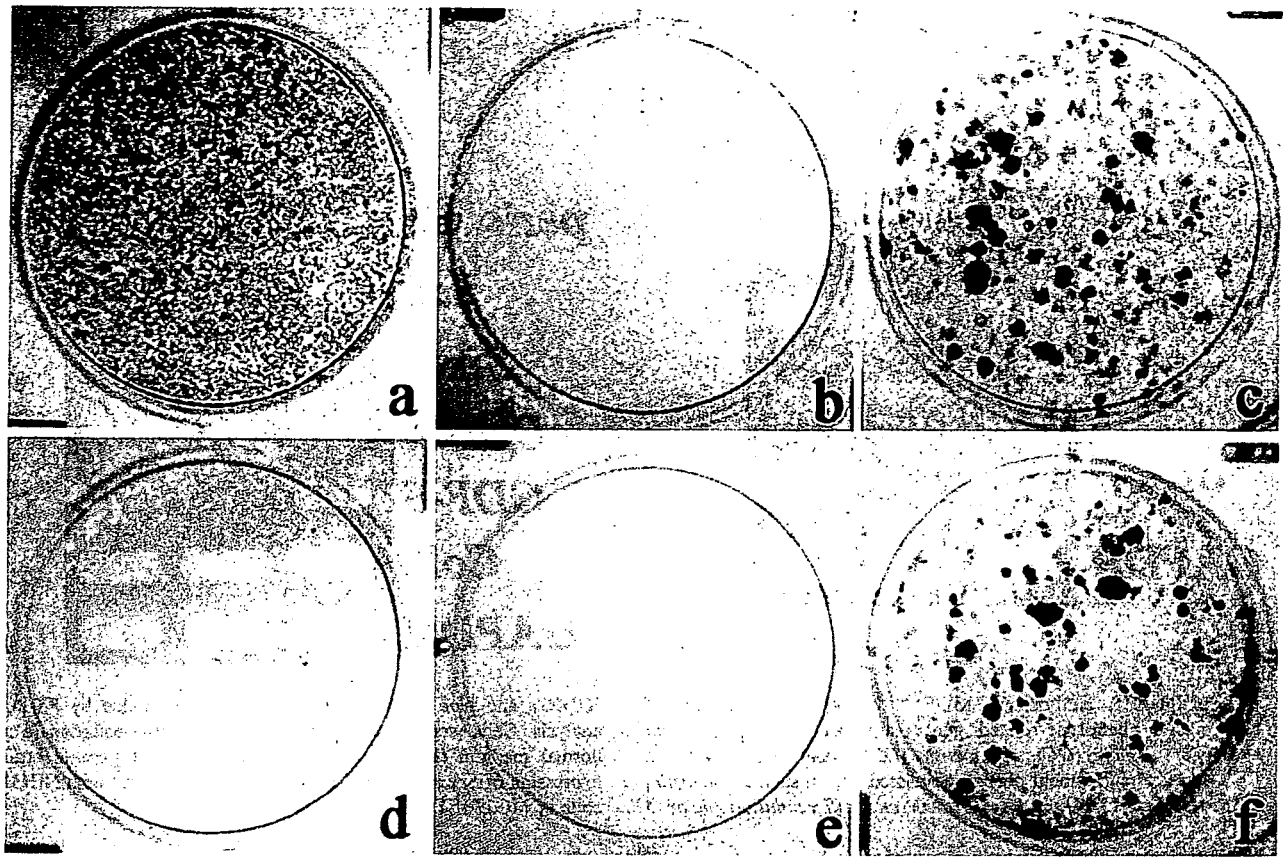

Fig. 2 ALP activity and mineralization potential of $MDF^{E6\text{-}EGFP}$ cells in vitro. $MDF^{E6\text{-}EGFP}$ cells were grown for 21 days in osteogenic differentiation medium in order to analyze ALP activity (**a–c**) and mineralization potential (**d–f**). High ALP activity by $MDF^{E6\text{-}EGFP}$ cells and MC3T3E1 (**a**, **c**) cells was apparent, whereas no activity was observed for NIH3T3 cells (**b**). Alizarin red staining showed no mineralized nodule formation for $MDF^{E6\text{-}EGFP}$ cells and NIH3T3 cells (**d**, **e**), whereas mineralized deposits were readily apparent for MC3T3E1 cells (**f**)

sections were blocked with 1% bovine serum albumin and probed with goat anti-type I collagen polyclonal antibody (Southern Biotech, Birmingham, Ala., USA) for 1 h. Sections were then probed with donkey anti-goat Alexa 555 (Invitrogen). After several washes, fluorescence in the sections was observed by fluorescence microscopy.

Results

Localization of periostin mRNA in the incisor tooth

Sequential developmental process of the dental follicle was observed in a sagittal section (in an anterior-posterior direction) of the P1 mice incisor (Fig. 1a). Immature cells were located posteriorly (Fig. 1c,e,g), and differentiation progressed toward the anterior region (Fig. 1b,d,f). To locate immature dental follicle cells, we first investigated the expression pattern of a PDL marker gene, *periostin*, and a cementoblast/osteoblast marker, *osteopontin*, in the lower incisor tooth germ of P1 mice. In a section stained with hematoxylin and eosin, dentin was seen in the anterior region (Fig. 1b), and invaginating dental epithelium was observed lingually in the posterior region (Fig. 1c). Intense expression of *periostin* was observed in the dental follicle cells close to the dentin layer in the anterior region (Fig. 1d, arrows). In contrast, only patchy expression of *periostin* was observed in the dental follicle cells in the posterior region (Fig. 1e, arrows). *Osteopontin* was expressed intensely throughout the alveolar bone (Fig. 1f,g, arrowheads). In accordance with the *periostin* expression pattern, *osteopontin* was expressed in the cementoblast adjacent to the dentin-forming layer in the anterior region (Fig. 1f, asterisks), but not in the posterior region (Fig. 1g). These data confirmed that the dental follicle cells in the posterior region were in an immature stage, whereas those in the anterior region were differentiated. We thus dissected dental follicle cells from the posterior region in order to establish a dental follicle progenitor cell culture system.

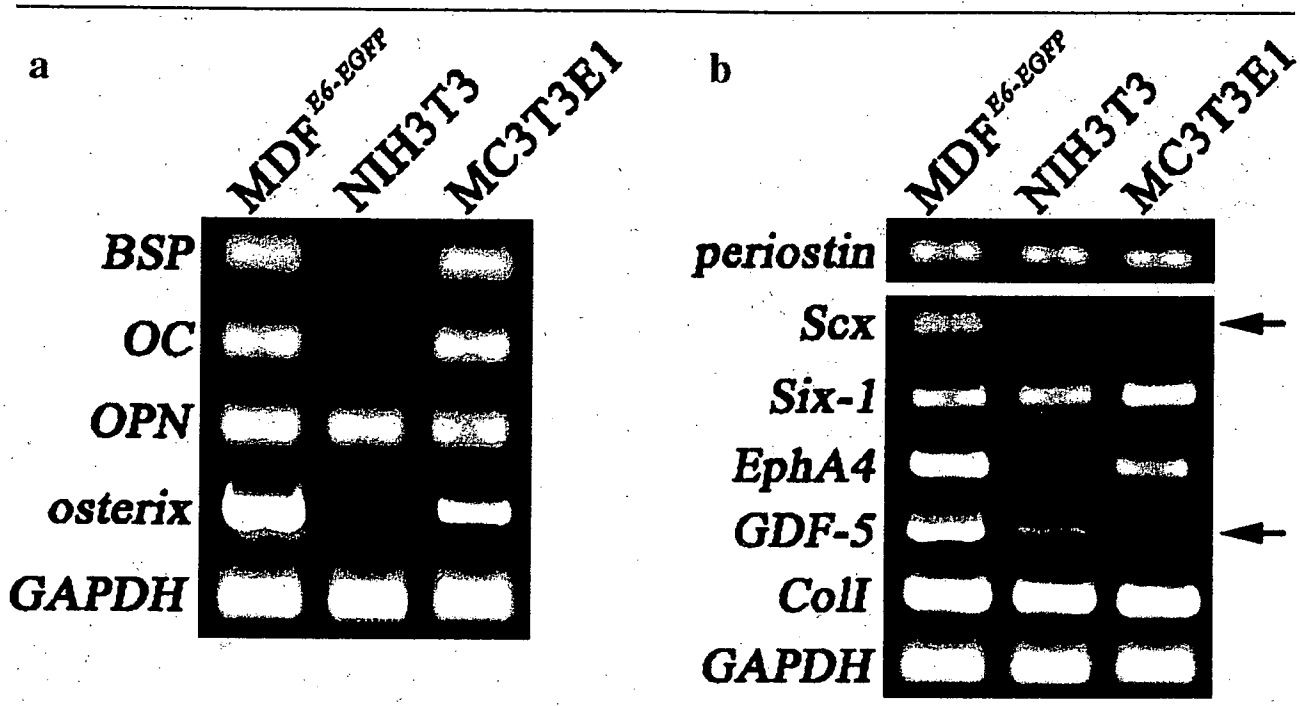

Fig. 3 RT-PCR analysis of $MDF^{E6\text{-}EGFP}$ cells. Expression of osteoblastic phenotype-related genes such as *bone sialoprotein* (*BSP*), *osteocalcin* (*OC*), *osteopontin* (*OPN*), and *osterix* (**a**), and PDL and tendon/ligament phenotype-related genes, such as *periostin*, *scleraxis* (*Scx*), *Six-1*, *EphA4*, *growth and differentiation factor 5* (*GDF5*), and *type I collagen* (*ColI*; **b**) were examined by RT-PCR analysis. Cells were cultured with osteoblastic differentiation (**a**) or normal medium (**b**), and total RNA was extracted (*arrows* strong expression of *Scx* and *GDF-5* in $MDF^{E6\text{-}EGFP}$ compared with NIH3T3 cells or MC3T3E1 cells)

Characterization of $MDF^{E6\text{-}EGFP}$ cells

MDF cells were isolated from the posterior region of the incisor tooth germ, and their life span was extended by using a retrovirus-expressing human papillomavirus type 16 (HPV16) *E6* gene lacking the PDZ-domain-binding motif ($E6^{\Delta 146\text{-}151}$), together with a lentivirus expressing *EGFP* for fluorescence detection. After viral infection, the expression of $E6^{\Delta 146\text{-}151}$ was confirmed by RT-PCR analysis (data not shown). $MDF^{E6\text{-}EGFP}$ cells maintained their original morphology and cell proliferation activity, even when the cells were cultured beyond population doubling (PD) 150, indicating that they had overcome replicative senescence. In contrast, normal MDF cells were only able to propagate until PD 10 (data not shown). We thus used $MDF^{E6\text{-}EGFP}$ cells for further analysis.

To assess the osteogenic potential of $MDF^{E6\text{-}EGFP}$ cells, the cells were treated with osteogenic differentiation medium supplemented with ascorbic acid, β-glycerophosphate, and dexamethasone for 21 days. ALP activity was observed in $MDF^{E6\text{-}EGFP}$ cells (Fig. 2a) and in osteoblast-like MC3T3E1 cells (Fig. 2c). Mineralized nodule formation by the $MDF^{E6\text{-}EGFP}$ cells was not observed (Fig. 2d), whereas MC3T3E1 cells were able to deposit mineralized nodules (Fig. 2f). Neither ALP activity nor mineral deposition was observed in the fibroblastic cells (NIH3T3 cells; Fig. 2b,e). RT-PCR analysis was performed to characterize the $MDF^{E6\text{-}EGFP}$ cells by using primers for osteoblast phenotype-related genes *BSP*, *OC*, and *osterix*. $MDF^{E6\text{-}EGFP}$ cells expressed all of these osteoblast marker genes, with a similar expression pattern to that of MC3T3E1 cells. In contrast, no expression of osteoblast phenotype-related genes was observed in NIH3T3 cells, except for *BSP*. From these data, we considered that osteoblastic populations were present in $MDF^{E6\text{-}EGFP}$ cells (Fig. 3a).

To characterize the PDL-forming properties of $MDF^{E6\text{-}EGFP}$ cells, gene expression of *periostin* and tendon/ligament phenotype-related genes encoding *Scx*, *EphA4*, *Six-1*, *GDF-5*, and *ColI* were examined by RT-PCR analysis. $MDF^{E6\text{-}EGFP}$ cells expressed all of these genes suggesting that they possessed PDL and tendon cell properties (Fig. 3b). Stronger expression of *Scx* and *GDF-5* was observed in $MDF^{E6\text{-}EGFP}$ cells than in NIH3T3 cells or MC3T3E1 cells (Fig. 3b, arrows). Expression patterns of *Scx* and *periostin* mRNA were examined in postnatal (P35) mouse molar PDL (Fig. 4a) by in situ hybridization. Intense expression of *periostin* was observed throughout the PDL (Fig. 4b, arrows), and *Scx* was also expressed in the PDL (Fig. 4c, arrowheads).

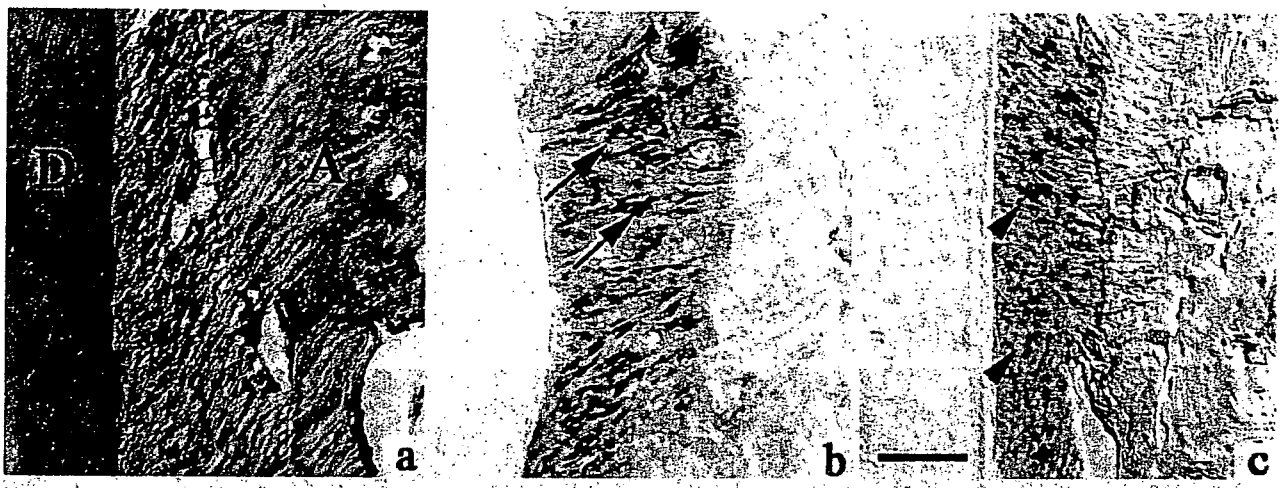

Fig. 4 In situ hybridization for *Scx* and *periostin* mRNA in postnatal PDL (*A* alveolar bone, *D* dentin, *P* PDL). Frontal sections of the molar tooth of P35 mouse (**a**) were examined by hematoxylin and eosin staining (**a**) or in situ hybridization with *periostin* (**b**) or *Scx* (**c**). Intense expression of *periostin* was seen within PDL (**b**, *arrows*). Expression of *Scx* can be seen throughout the PDL (**c**, *arrowheads*). *Bars* 100 μm

In vivo characterization of $MDF^{E6\text{-}EGFP}$ cells

To investigate the differentiation potential of $MDF^{E6\text{-}EGFP}$ cells, the cells were implanted into SCID mice. After 4 weeks, MDFE6-EGFP cell transplants formed PDL-like fibrous tissue (Fig. 5a-a) including scattered bone-like tissue formation (Fig. 5a-b). The PDL-like tissues resembled the structure of PDL with sheet-like cells (Fig. 5a-a, a-d, arrows). Cells within the PDL- and bone-like tissues were strongly positive for EGFP (Fig. 5a-d, a-e). In contrast, no such tissues were formed in the transplants without mouse cells (HAP transplants; Fig. 5a-f). Immunohistochemical staining revealed dense type I collagen fibril assembly in the PDL-like tissue (Fig. 5b-a), whereas type I collagen fibril assembly was not evident in the NIH3T3 cell or HAP transplants (Fig. 5b-b, b-c). To validate the capacity of $MDF^{E6\text{-}EGFP}$ cells to differentiate into PDL in vivo, the expression of *periostin* and *Scx* was examined in the transplants by in situ hybridization. Expression of *type XII collagen* has been shown in the PDL during tooth root formation; therefore, we also examined the expression of this gene in the transplants (MacNeil et al. 1998). As expected, the expression of *periostin*, *Scx*, and *type XII collagen* was observed in $MDF^{E6\text{-}EGFP}$ cells (Fig. 6a,d,g, arrows), whereas these genes were not expressed in the NIH3T3 cell transplants (Fig. 6b,e,h) or HAP transplants (Fig. 6c,f,i). All the transplants except HAP transplants were EGFP-positive, indicating that cells within the $MDF^{E6\text{-}EGFP}$ and NIH3T3 transplants had originated from the donor (Fig. 6j,k,l).

Discussion

We have immortalized dental follicle cells from cells isolated from mice incisor tooth germs. These cells express *Scx*, *GDF-5*, *EphA4*, *Six-1*, and *Coll*, which are expressed in a developing tendon (Bonnin et al. 2005; Brent et al. 2003; Luukko et al. 2005; Settle et al. 2003). Our findings also suggest that $MDF^{E6\text{-}EGFP}$ cells act as PDL progenitors since they form a PDL-like structure that expresses *periostin*, *Scx*, and *type XII collagen* and that is capable of producing dense collagen fibril assembly in vivo.

In the present study, $MDF^{E6\text{-}EGFP}$ cells have been isolated from the undifferentiated dental follicle region of the incisor in which there is minimal expression of *periostin* and no expression of *osteopontin*. Our findings indicate that $MDF^{E6\text{-}EGFP}$ cells act as PDL progenitors, as shown by their capacity to generate PDL-like tissue in vivo. $MDF^{E6\text{-}EGFP}$ cells are similar to tendon progenitors with respect to their expression of *Scx* and *GDF-5*, a marker for tendon/ligament. Since PDL is morphologically similar to the tendon/ligament in vivo, dental follicle cells may have a similar phenotype as tendon progenitors. The expression of *Scx* by mouse PDL has been seen in the present study, suggesting that the PDL has some characteristics similar to tendon. Salingcamboriboon and coworkers (2003) have reported that a tendon-derived cell line isolated from mouse Achilles tissue shows expression of *Scx*, and that these cells are able to form tendon-like tissue when they are implanted into a mouse tendon-defect model. $MDF^{E6\text{-}EGFP}$ cells show a similar phenotype to these cells, and the transplants form PDL-like tissues comprising cells

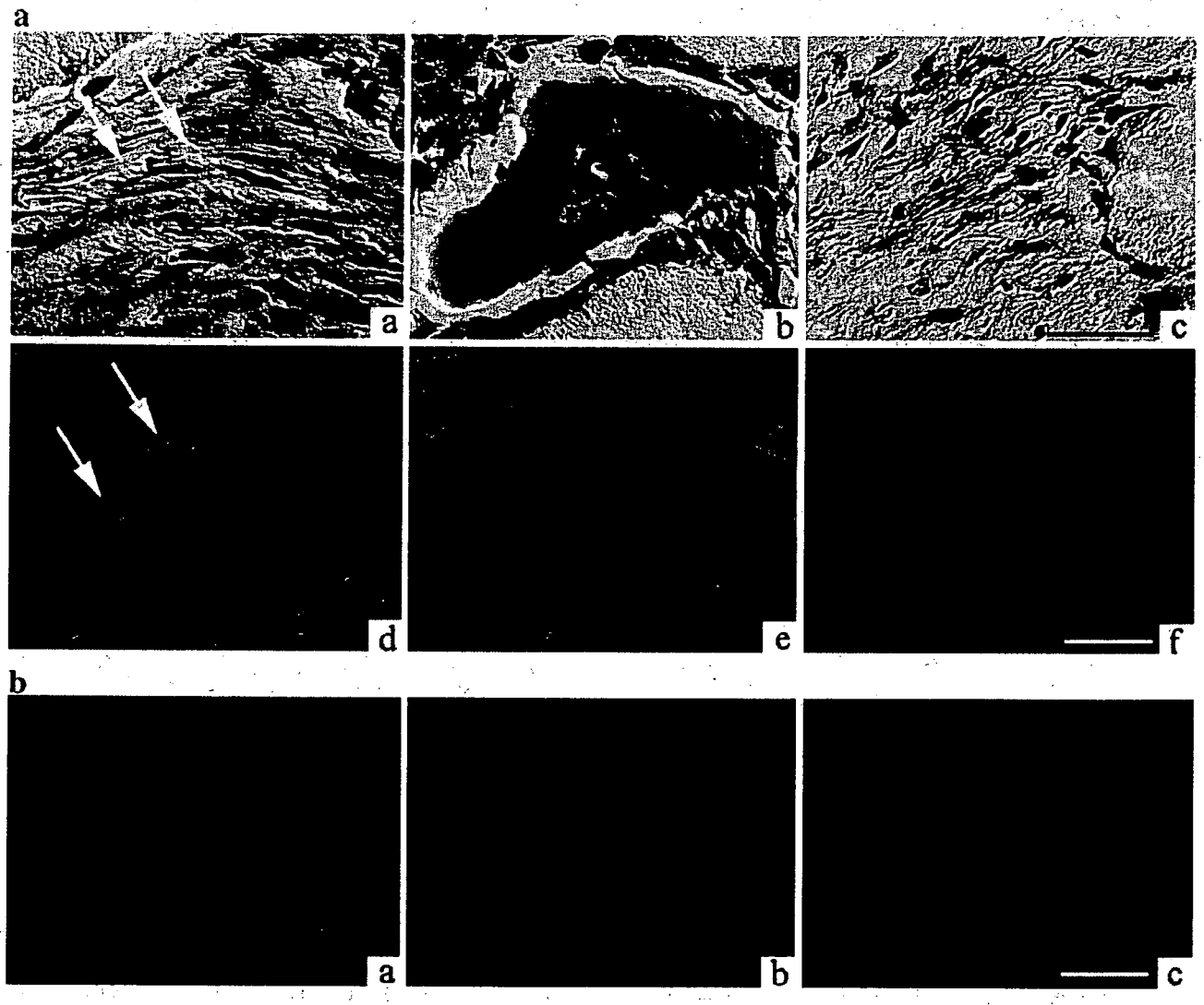

Fig. 5 Differentiation potential of $MDF^{E6\text{-}EGFP}$ cells in vivo. **a** Representative sections of $MDF^{E6\text{-}EGFP}$ cell transplants (**a-a**, **a-b**, **a-d**, and **a-e**) and transplants without mouse cells (HAP transplants; **a-c**, **a-f**). The transplant was stained with hematoxylin and eosin (**a–a** to **a-c**) or viewed for EGFP fluorescence (**a-d** to **a-f**). PDL-like fibrous tissues (**a-a**, **a-d**, *arrows*) and bone-like tissues (**a-e**) are visible in the $MDF^{E6\text{-}EGFP}$ transplants. Cells within the $MDF^{E6\text{-}EGFP}$ transplants are positive for EGFP (**a-d**, **a-e**). **b** Immunohistochemical staining with anti-type I collagen polyclonal antibody in the $MDF^{E6\text{-}EGFP}$ transplants (**b-a**), NIH3T3 cell transplants (**b-b**), or HAP transplants (**b-c**) are shown. Dense type I collagen fibril assemblies are seen in the $MDF^{E6\text{-}EGFP}$ transplants. *Bars* 50 μm

with sheet-like extensions surrounding a densely packed, collagen fibril assembly. Our data are also coincident with previous findings that human PDL cells are able to form PDL-like tissue upon implantation into immunodeficient mice for 4 weeks, suggesting that the differentiation potential of $MDF^{E6\text{-}EGFP}$ is comparable with these cells (Grzesik et al. 2000; Seo et al. 2004). In the present study, the PDL differentiation of $MDF^{E6\text{-}EGFP}$ cells has been assessed by the expression of *periostin*, *Scx*, and *type XII collagen* (Bohme et al. 1995; Karimbux and Nishimura 1995). The expression of *periostin* is observed in both alveolar bone cells and dental follicle cells on P1. However, previous findings and our data have shown that the expression of *periostin* is limited to the adult periodontal ligament, indicating that it could be used as a marker for differentiated PDL (Kruzynska-Frejtag et al. 2004). In the case of $MDF^{E6\text{-}EGFP}$ transplants, they form PDL-like tissue expressing *periostin*, *Scx*, and *type XII collagen*, thus indicating that the tissue is almost identical to PDL. From these findings, we suggest that the $MDF^{E6\text{-}EGFP}$ cells have PDL progenitors able to differentiate into PDL in vivo. Although the role of the tendon/ligament related genes in PDL development is not clear, these data strongly support our hypothesis that $MDF^{E6\text{-}EGFP}$ cells possess PDL progenitors that resemble tendon progenitors.

Progenitors for cementoblasts, PDL cells, and osteoblasts are generally believed to be present in dental follicle cells (Ten Cate 1994), and we have previously shown that

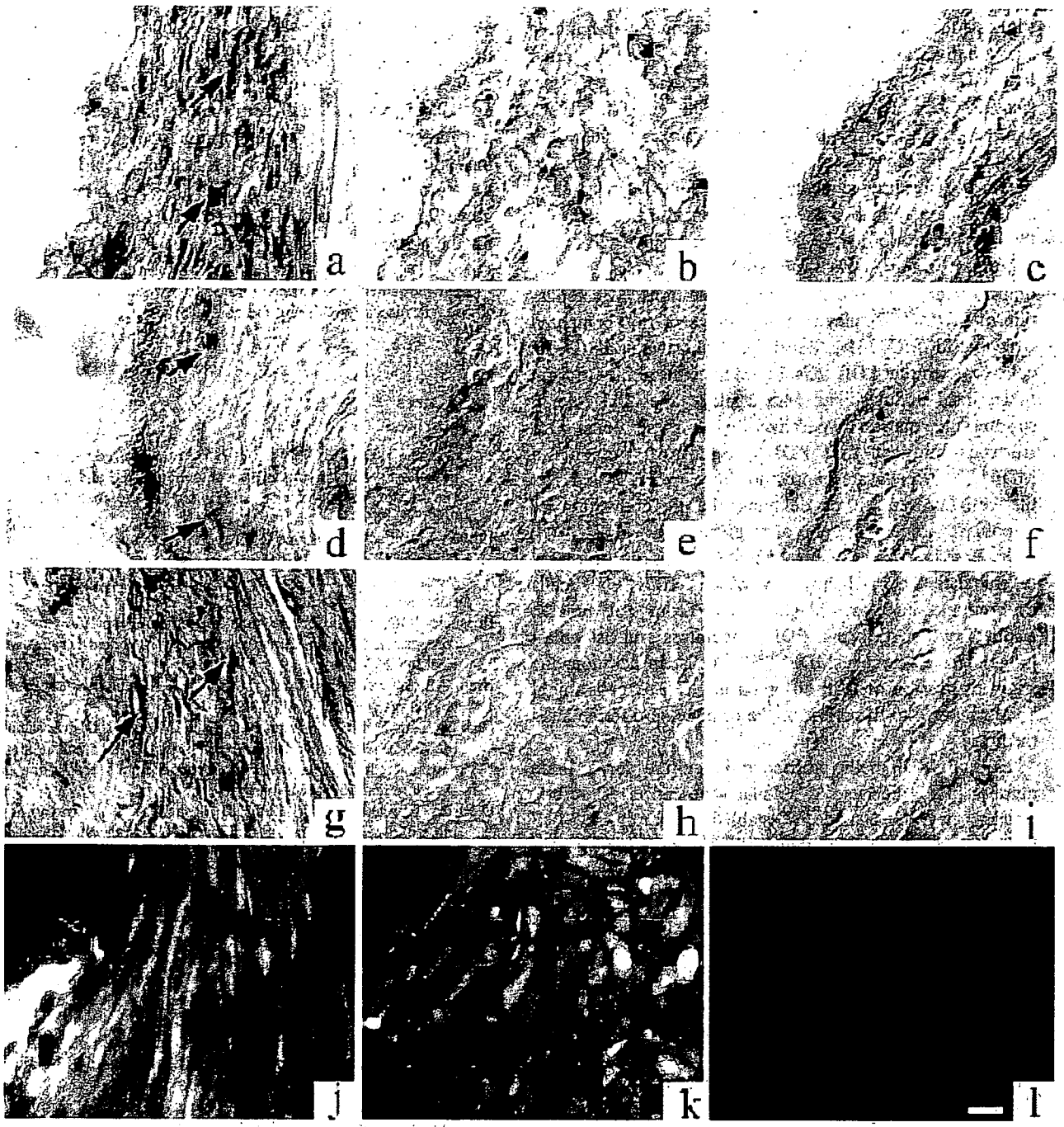

Fig. 6 In situ hybridization for *periostin*, *Scx*, and *type XII collagen* mRNA in $MDF^{E6\text{-}EGFP}$ cell transplants. Representative sections of $MDF^{E6\text{-}EGFP}$ cell transplants (**a**, **d**, **g**, **j**), NIH3T3 cell transplants (**b**, **e**, **h**, **k**), and transplants without mouse cells (HAP transplants; **c**, **f**, **i**, **l**) were analyzed by in situ hybridization for *periostin* (**a–c**), *Scx* (**d–f**), or *type XII collagen* (**g–i**), or viewed for EGFP fluorescence (**j–l**). Expression of *periostin*, *Scx*, or *type XII collagen* is seen in the $MDF^{E6\text{-}EGFP}$ transplants (**a**, **d**, **g**, *arrows*). Cells within the $MDF^{E6\text{-}EGFP}$ and NIH3T3 transplants are positive for EGFP (**j**, **k**). *Bar* 100 μm

cementoblast progenitors can be obtained from bovine dental follicle tissues (Handa et al. 2002). Cementoblast differentiation does not occur in $MDF^{E6\text{-}EGFP}$ cell transplants. This discrepancy may be explained by the isolation technique used for $MDF^{E6\text{-}EGFP}$ cells. The cells grown from mouse dental follicle tissues have been employed in this study, whereas in a previous study, we isolated bovine dental follicle cells by bacterial collagenase digestion; this

suggests that isolation of cementoblast progenitors requires enzyme digestion (Handa et al. 2002). We have also found that $MDF^{E6\text{-}EGFP}$ cells can act as osteoblast progenitors, since they form bone-like tissue in vivo. Although $MDF^{E6\text{-}EGFP}$ cells express an array of osteoblast marker genes, they cannot form mineralized nodules in vitro, as described previously for bovine dental follicle cells (Handa et al. 2002). This may be because the difference in time required for the calcification of MDF^{E6EFGP}. The timing and extent of mineralization varies substantially depending on the origin of the cells or experimental conditions. Mineralization of MDF^{E6EFGP} may require a longer period compared with that for MC3T3E1. Recently, Yoshizawa et al. (2004) have reported that PDL cells do not have the ability to form mineralized nodules, and Msx-2 plays a central role in suppressing matrix mineralization in these cells. Our findings suggest that PDL progenitors present in $MDF^{E6\text{-}EGFP}$ cells are similar to those in PDL, and that the cells preventing or delaying the mineralization of osteoblast progenitors are also present in $MDF^{E6\text{-}EGFP}$ cells. Based on these findings, future studies are necessary to elucidate the mechanism by which $MDF^{E6\text{-}EGFP}$ cells differentiate into osteoblastic cells. From our present findings, we suggest that PDL progenitors and osteoblast progenitors co-exist in $MDF^{E6\text{-}EGFP}$ cells. In addition, the slight expression of BSP observed in NIH3T3 cells might be attributable to the effect of the osteogenic differentiated medium.

Normal MDF cells proliferate in culture for a finite number of PD because of cellular senescence. Therefore, attempts have been made to establish immortalized MDF cells in order to analyze their differentiation potential. A deficiency in p53 is sufficient for the establishment of mouse clonal cell lines from various tissues (Hanazono et al. 1997). HPV16E6 has been shown to abrogate the function of p53 and has the ability to immortalize various cell types (Fehrmann and Laimins 2003; Kiyono et al. 1998). However, it also has other biological functions that depend on its C-terminal PDZ-domain-binding motif, such as cell transformation and skin hyperplasia in transgenic mice (Nguyen et al. 2003). For instance, mice expressing HPV-16 E6 in their epidermis develop epithelial hyperplasia and squamous carcinomas (Song et al. 1999). However, transgenic mice expressing HPV-16 E6 lacking the PDZ-binding motif fail to display epithelial hyperplasia but retain the ability to inactivate p53 (Nguyen et al. 2003). In the present study, we have used a mutant version of E6 that lacks the C-terminal PDZ-domain binding-motif to extend the life span of MDF cells and have succeeded in immortalizing MDF cells without affecting their differentiation potential. In addition, we have confirmed that no tumor formation occurs in $MDF^{E6\text{-}EGFP}$ cell transplants (data not shown). This suggests that the immortalization system used in this study might be useful for the immortalization of MDF cells.

In summary, we have established an immortalized mouse dental follicle cell culture system that possesses PDL progenitors. $MDF^{E6\text{-}EGFP}$ cells might provide new insights into the mechanisms of PDL formation, including those pertaining to PDL cell differentiation. They may also be a powerful tool in the development of therapeutic strategies for the treatment of periodontitis.

Acknowledgement We are grateful to Dr. Masato Yamauchi for his advice and discussions during the course of this work.

References

Bohme K, Li Y, Oh PS, Olsen BR (1995) Primary structure of the long and short splice variants of mouse collagen XII and their tissue-specific expression during embryonic development. Dev Dyn 204:432–445

Bonnin MA, Laclef C, Blaise R, Eloy-Trinquet S, Relaix F, Maire P, Duprez D (2005) Six1 is not involved in limb tendon development, but is expressed in limb connective tissue under Shh regulation. Mech Dev 122:573–585

Bosshardt DD, Schroeder HE (1996) Cementogenesis reviewed: a comparison between human premolars and rodent molars. Anat Rec 245:267–292

Brent AE, Schweitzer R, Tabin CJ (2003) A somitic compartment of tendon progenitors. Cell 113:235–248

Chai Y, Jiang X, Ito Y, Bringas P Jr, Han J, Rowitch DH, Soriano P, McMahon AP, Sucov HM (2000) Fate of the mammalian cranial neural crest during tooth and mandibular morphogenesis. Development 127:1671–1679

D'Errico JA, Ouyang H, Berry JE, MacNeil RL, Strayhorn C, Imperiale MJ, Harris NL, Goldberg H, Somerman MJ (1999) Immortalized cementoblasts and periodontal ligament cells in culture. Bone 25:39–47

Fehrmann F, Laimins LA (2003) Human papillomaviruses: targeting differentiating epithelial cells for malignant transformation. Oncogene 22:5201–5207

Grzesik WJ, Cheng H, Oh JS, Kuznetsov SA, Mankani MH, Uzawa K, Robey PG, Yamauchi M (2000) Cementum-forming cells are phenotypically distinct from bone-forming cells. J Bone Miner Res 15:52–59

Hanazono M, Tomisawa H, Tomooka Y, Hirabayashi K, Aizawa S (1997) Establishment of uterine cell lines from p53-deficient mice. In Vitro Cell Dev Biol Anim 33:668–671

Handa K, Saito M, Yamauchi M, Kiyono T, Sato S, Teranaka T, Sampath Narayanan A (2002) Cementum matrix formation in vivo by cultured dental follicle cells. Bone 31:606–611

Horiuchi K, Amizuka N, Takeshita S, Takamatsu H, Katsuura M, Ozawa H, Toyama Y, Bonewald LF, Kudo A (1999) Identification and characterization of a novel protein, periostin, with restricted expression to periosteum and periodontal ligament and increased expression by transforming growth factor beta. J Bone Miner Res 14:1239–1249

Iseki S, Wilkie AO, Morriss-Kay GM (1999) Fgfr1 and Fgfr2 have distinct differentiation- and proliferation-related roles in the developing mouse skull vault. Development 126:5611–5620

Karimbux NY, Nishimura I (1995) Temporal and spatial expressions of type XII collagen in the remodeling periodontal ligament during experimental tooth movement. J Dent Res 74:313–318

Kiyono T, Foster SA, Koop JI, McDougall JK, Galloway DA, Klingelhutz AJ (1998) Both Rb/p16INK4a inactivation and telomerase activity are required to immortalize human epithelial cells. Nature 396:84–88

Kruzynska-Frejtag A, Wang J, Maeda M, Rogers R, Krug E, Hoffman S, Markwald RR, Conway SJ (2004) Periostin is expressed within the developing teeth at the sites of epithelial-mesenchymal interaction. Dev Dyn 229:857–868

Kyo S, Nakamura M, Kiyono T, Maida Y, Kanaya T, Tanaka M, Yatabe N, Inoue M (2003) Successful immortalization of endometrial glandular cells with normal structural and functional characteristics. Am J Pathol 163:2259–2269

Luukko K, Loes S, Kvinnsland IH, Kettunen P (2005) Expression of ephrin-A ligands and EphA receptors in the developing mouse tooth and its supporting tissues. Cell Tissue Res 319:143–152

MacNeil RL, Berry JE, Strayhorn CL, Shigeyama Y, Somerman MJ (1998) Expression of type I and XII collagen during development of the periodontal ligament in the mouse. Arch Oral Biol 43: 779–787

Matias MA, Li H, Young WG, Bartold PM (2003) Immunohistochemical localisation of extracellular matrix proteins in the periodontium during cementogenesis in the rat molar. Arch Oral Biol 48:709–716

Morotome Y, Goseki-Sone M, Ishikawa I, Oida S (1998) Gene expression of growth and differentiation factors-5, -6, and -7 in developing bovine tooth at the root forming stage. Biochem Biophys Res Commun 244:85–90

Nakamura T, Yamamoto M, Tamura M, Izumi Y (2003) Effects of growth/differentiation factor-5 on human periodontal ligament cells. J Periodontal Res 38:597–605

Nguyen ML, Nguyen MM, Lee D, Griep AE, Lambert PF (2003) The PDZ ligand domain of the human papillomavirus type 16 E6 protein is required for E6's induction of epithelial hyperplasia in vivo. J Virol 77:6957–6964

Rios H, Koushik SV, Wang H, Wang J, Zhou HM, Lindsley A, Rogers R, Chen Z, Maeda M, Kruzynska-Frejtag A, Feng JQ, Conway SJ (2005) Periostin null mice exhibit dwarfism, incisor enamel defects, and an early-onset periodontal disease-like phenotype. Mol Cell Biol 25:11131–11144

Saito M, Handa K, Kiyono T, Hattori S, Yokoi T, Tsubakimoto T, Harada H, Noguchi T, Toyoda M, Sato S, Teranaka T (2005) Immortalization of cementoblast progenitor cells with Bmi-1 and TERT. J Bone Miner Res 20:50–57

Salingcarnboriboon R, Yoshitake H, Tsuji K, Obinata M, Amagasa T, Nifuji A, Noda M (2003) Establishment of tendon-derived cell lines exhibiting pluripotent mesenchymal stem cell-like property. Exp Cell Res 287:289–300

Sena K, Morotome Y, Baba O, Terashima T, Takano Y, Ishikawa I (2003) Gene expression of growth differentiation factors in the developing periodontium of rat molars. J Dent Res 82:166–171

Seo BM, Miura M, Gronthos S, Bartold PM, Batouli S, Brahim J, Young M, Robey PG, Wang CY, Shi S (2004) Investigation of multipotent postnatal stem cells from human periodontal ligament. Lancet 364:149–155

Settle SH Jr, Rountree RB, Sinha A, Thacker A, Higgins K, Kingsley DM (2003) Multiple joint and skeletal patterning defects caused by single and double mutations in the mouse Gdf6 and Gdf5 genes. Dev Biol 254:116–130

Song S, Pitot HC, Lambert PF (1999) The human papillomavirus type 16 E6 gene alone is sufficient to induce carcinomas in transgenic animals. J Virol 73:5887–5893

Ten Cate AR (1994) Oral histology, development, structure, and function, 4th edn. Mosby, St. Louis

Wilkinson DG (1995) RNA detection using non-radioactive in situ hybridization. Curr Opin Biotechnol 6:20–23

Wolfman NM, Hattersley G, Cox K, Celeste AJ, Nelson R, Yamaji N, Dube JL, DiBlasio-Smith E, Nove J, Song JJ, Wozney JM, Rosen V (1997) Ectopic induction of tendon and ligament in rats by growth and differentiation factors 5, 6, and 7, members of the TGF-beta gene family. J Clin Invest 100:321–330

Yoshizawa T, Takizawa F, Iizawa F, Ishibashi O, Kawashima H, Matsuda A, Endo N, Kawashima H (2004) Homeobox protein MSX2 acts as a molecular defense mechanism for preventing ossification in ligament fibroblasts. Mol Cell Biol 24:3460–3472

Expert Opinion

informa
healthcare

Oncologic, Endocrine & Metabolic

Molecular mechanisms of cellular senescence and immortalization of human cells

Tohru Kiyono
National Cancer Center Research Institute, Virology Division, 5-1-1 Tsukiji, Chuo-ku, Tokyo 104-0045, Japan

Cellular senescence was originally described as a phenomenon observed in cultured human cells. Accumulating lines of evidence now indicate that the same processes also take place *in vivo*, suggesting important implications for tumor development. Telomere shortening is the most well-established cause of cellular senescence that can be induced by many other intrinsic and extrinsic factors. The retinoblastoma susceptibility gene product is a convergent target that is downstream of these factors. p53, p38MAPK and cyclin-dependent kinase inhibitors p16INK4a (p16) and p21CIP1 (p21) are key mediators. As most stresses that induce cellular senescence are also known causes of cancer, a common strategy might be applied to the development of cancer chemopreventive agents and anti-ageing drugs.

Keywords: ageing, cyclin-dependent kinase, cyclin-dependent kinase inhibitor, immortalization, p16(INK4a), p21(WAF1/CIP1/SDI1), p38(MAPK), p53, polycomb group, reactive oxygen species, retinoblastoma protein, senescence, senescence-associated heterochromatic foci, telomerase reverse transcriptase, telomere

Expert Opin. Ther. Targets (2007) 11(12):1623-1637

1. Introduction

Most human cells undergo a limited number of divisions in culture and then enter a non-dividing state termed replicative senescence [1]. Unlike the case with quiescent cells, growth arrest of senescent cells is essentially irreversible and insensitive to growth factors. Cellular senescence refers to replicative senescence and replicative senescence-like states which can be induced by many stresses, such as genotoxic damage and active oncogenes. Activation of the retinoblastoma susceptibility gene product (pRb) is the most common downstream event of many senescing signals, though the other pRb family pocket proteins (p130 and p107) may substitute this function in the absence of pRb. pRb is inactivated by phosphorylation by cyclin-dependent kinases (CDKs) which are inactivated by CDK inhibitors. Induction of CDK inhibitors p16INK4a (p16) and p21CIP1 (p21), along with the activation of p53, are often associated with cellular senescence. By inhibiting CDKs, these inhibitors consequently activate pRb, which induces growth arrest at G1. Cdk4/Cdk6–cyclin D and Cdk2–cyclin E function as the major pRb kinases and mouse embryonic fibroblast (MEF) cells derived from double knockout of Cdk4 and Cdk2 feature early onset senescence [2], although a recent report indicated that Cdk1 can associate with all the cyclins and is the only essential Cdk for cell cycling ([3,4] for review). In contrast, overexpression of Cdk4/Cdk6 can delay cellular senescence [5]. In senescent cells, cell cycle arrest can be maintained by sustained growth arrest signaling and/or heterochromatinization of cell cycle-associated genes. There are numbers of intrinsic and extrinsic factors that induce cellular senescence; the same signaling pathway is often involved, although some of the underlying mechanisms are specific to the cell type and

the inducer. In this review, processes contributing to cellular senescence induced by different factors and their significance for human health are discussed.

2. Telomere shortening and senescence

Telomere shortening is the most well-known cause of cellular senescence or replicative senescence. In the absence of telomerase activity, telomeres are continuously shortened following replication, due to the 'end-replication problem' [6]. The shortened telomeres are exposed as linear ends of double strand DNAs and are recognized as a type of DNA damage. Dysfunction of shelterin, a multimolecular complex that regulates telomere length and protects telomere ends, could also lead to cellular senescence ([7] for review). Based on the notion that most human somatic cells lack telomerase activity, telomere shortening is considered to be a molecular clock that determines cellular ageing. Although some human somatic stem cells express higher levels of telomerase, the activity is not sufficient to maintain telomere length. Therefore, the clock theoretically limits the maximum replicative capacity of human cells. Indeed, some human cell types can be immortalized by transduction of human telomerase reverse transcriptase (hTERT) alone [8].

However, the situation changes in cells with high telomerase activity. Mouse cells have relatively long telomeres and expression of telomerase is more ubiquitous. The observed 'replicative senescence' in MEF culture is not caused by telomere shortening and, therefore, is called premature senescence or culture shock [9].

3. Telomere-independent senescence

Telomere-independent senescence can be induced, not only in cell culture but also *in vivo*, due to many kinds of stresses and is known by different names in different situations, such as premature senescence, stress-induced premature senescence, culture shock and stress or aberrant signaling induced senescence to distinguish it from telomere-dependent senescence or replicative senescence [9,10]. However, telomere shortening or dysfunction itself is a stress to cells. The p53 and pRb pathways are common regulators that govern both telomere-dependent and -independent senescence. Furthermore, the term cellular senescence arose from the assumption that similar mechanisms of cellular ageing occur in both culture and *in vivo*, and the telomere-dependent and -independent forms of senescence could be equally important as biologic mechanisms to suppress tumor formation. Indeed, the observed cellular senescence is likely to be frequently induced by the sum of telomere-dependent and telomere-independent stresses. Therefore, the term replicative senescence in many papers refers to phenomena observed in culture, rather than being based on any mechanistic concept. To indicate mechanistic features of senescence, terms, such as telomere-dependent and oncogene-induced senescence are used in the present review.

4. DNA damage response and senescence

Many types of DNA damage have been identified as inducers of senescence, as well as apoptosis. In the case of telomere-dependent senescence, continuous growth arrest signals from shortened telomeres are causes. However, slight DNA damage induces transient cell cycle arrest followed by DNA repair, which then allows cells to re-enter the cell cycle. Therefore, relatively heavy or continuous DNA damage is generally chosen for experimental induction of senescence. Genotoxic stress due to reactive oxygen species (ROS), UV, γ-rays and DNA-damaging agents, including chemotherapeutic drugs, have been reported as inducing agents (**Figure 1**) ([11] for review). DNA damage results in activation of ataxia-telangiectasia mutation (ATM), p53 and subsequently, many p53 target genes, including *p21*. Depending on the cell type and the extent of DNA damage, activation of p53 induces either apoptosis or senescence. It has been suggested that *p21* plays a critical role in both inducing p53-dependent senescence and protecting against apoptosis [12-15]. Induction of p21 prevents cells from accumulating further damage by inducing growth arrest through an association with cyclin/CDKs and proliferating cell nuclear antigen, thereby providing time for repair to be accomplished.

5. Reactive oxygen species-induced senescence of mouse embryonic fibroblast cells

Replicative senescence is caused by shortened telomeres in human foreskin fibroblasts. However, primary MEF cells also enter senescence prematurely, independent of telomere length after several passages, as they have long telomeres and often express TERT. Cellular senescence of MEF was, thus, suggested to be caused by 'culture shock' [9] and later shown to be caused by ROS in the widely used carbon dioxide incubators, which contain a higher atmospheric oxygen concentration (20.8%) than that in the tissue environment [16]. As similar senescence of human foreskin fibroblasts can be induced by hydrogen peroxide, it is safe to say that the difference is based on relative sensitivity to ROS between human and mouse cells, and 'spontaneous' senescence of MEF cells should be interpreted as 'ROS-induced senescence'. Therefore, MEF cells can be essentially considered as immortal at lower oxygen concentrations (3%), and examples lacking p53, $p19^{Arf}$, inducer of acute promyelocytic leukemia (PML) or all the pRb family proteins (pRb, p107 and p130) are resistant to 'ROS-induced senescence' and Ras-induced senescence. However, it remains to be examined whether mouse cells derived from different tissues are also virtually immortal with low oxygen concentrations (3%) or in the presence of antioxidants. Similar effects of low oxygen conditions on human diploid cells were reported 30 years ago [17].

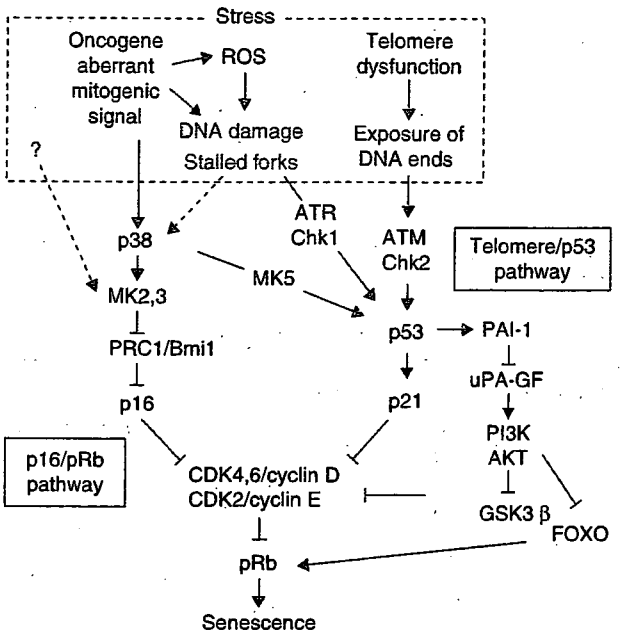

Figure 1. Major pathways to induce cellular senescence. Many stresses can induce cellular senescence. In this model, telomere dysfunction including telomere shortening, is also classified as a stress. The PI3K/Akt pathway can be suppressed by negative feedback signaling, originally triggered by activation of the Raf/MEK/ERK pathway.
ATM: Ataxia-telangiectasia mutation; ATR: Ataxia-telangiectagia and rad3-related; CDK: Cyclin-depedent kinase; Chk1: Cell cycle checkpoint kinase 1; FOXO: Forkhead transcription factor; GF: Growth factor; GSK: Glycogen synthase kinase; MK: MAPK activated protein kinase; PAI: Plasminogen activator inhibitor 1; PRC: Polycomb repressor complexes; pRb: Retinoblastoma protein; ROS: Reactive oxygen species; uPA: Urokinase-type plasminogen activator.

6. Oncogene-induced senescence

Oncogene-induced senescence (OIS) was first reported as an *in vitro* phenomenon in response to oncogenic Ras and Raf [10,18]. Both p53 activation and p16 elevation are induced in OIS, although changes in p16 appears to be less important in senescence of mouse cells [19,20]. Several common and specific mechanisms are proposed for OIS induced by different oncogenes. P14ARF is specifically activated by aberrant expression of E2F through a non-typical, E2F-responsive element in the promoter [21]. Independent of the E2F pathway, activation of Arf by Ras/Raf signaling is also indirectly mediated by Dmp1 through activation of Jun, explaining why Dmp1 null primary cells are highly susceptible to Ras-induced transformation [22]. p14ARF induces accumulation of p53 through inhibition of the human homolog of murine double minute 2 (HDM2), although p53 is activated by oncogenic Ras, independent of p14ARF in some human cells [23].

In animal models of OIS, most cells expressing oncogenic Kras neither form tumors nor enter senescence [24]. Similarly, endogenous oncogenic KrasG12D-expressing fibroblasts do not enter senescence, but demonstrate attenuation and altered regulation of canonical Ras effector signaling pathways [25]. Such attenuation is caused by a global negative feedback response induced by mutations affecting neurofibromin, a Ras GTPase activating protein (RasGAP), Raf and Ras [26]. This negative feedback program is regulated in part by Ras guanine-nucleotide exchange factors, sprouty proteins, RasGAPs and MAPK phosphatases also called dual specificity phosphatises (DUSPs). Their inhibitory signals can suppress the PI3K/AKT pathway, which can exert an impact on the senescence pathway through forkhead transcription factor and HDM2 (Figure 1) [26]. Expression of a constitutively activated mutant of forkhead transcription factor 1 (FOXO1) can rapidly induce cellular senescence with activation of pRb, but not p53 [26]. Inhibition of HDM2 results in activation of p53. As a p53 downstream target, PAI-1, can also inhibit the PI3K/Akt pathway and induce senescence in the absence of p53 [27], PAI-1 might be involved in negative feedback loops. Recently, it was suggested that OIS is also a DNA damage response triggered by DNA hyper-replication, associated with overexpression of CDC6 and an increased number of active replicons [28,29]. The DNA damage response requires DNA replication, as oncogenic ras expression does not induce DNA damage in quiescent cells. DNA damage in OIS could be induced by ROS. Activation of the p16–Rb pathway in cooperation with mitogenic signals causes elevated intracellular levels of ROS, thereby activating PKCδ in human senescent cells [30]. Importantly, once activated by ROS, PKCδ promotes further generation of ROS by activating NADPH oxidase, thus, establishing a positive feedback loop to sustain ROS–PKCδ signaling [30].